Title
Using geodetic data in geothermal areas

Journal
The Leading Edge, 39(12)

ISSN
1070-485X

Authors
Vasco, Donald W
Rutqvist, Jonny
Jeanne, Pierre
et al.

Publication Date
2020-12-01

DOI
10.1190/tle39120883.1

Peer reviewed

Using Geodetic Data in Geothermal Areas

Donald W. Vasco[1], Jonny Rutqvist[1], Pierre Jeanne[1], Sergey V. Samsonov[2], and Craig Hartline[3]

[1] Energy Geosciences Division, Lawrence Berkeley National Laboratory, University of California, Berkeley, CA, USA e-mail: dwvasco@lbl.gov

[2] Canada Centre for Mapping and Earth Observation, Natural Resources Canada, Ottawa, ON, Canada

[3] Calpine Corporation, 10350 Socrates Mine Road, Middletown, CA 95461

Abstract

Geodetic observations, often in conjunction with other data, provide a cost-effective means for identifying and characterizing geothermal resources. A review of the various methods reveals how the technology for measuring deformation has advanced considerably in the past few decades. Currently, Interferometric Synthetic Aperture Radar (InSAR) is the method of choice for monitoring deformation at a geothermal field. A discussion of geodetic monitoring at The Geysers geothermal field, California, illustrates some of the progress made and the challenges that remain.

Introduction

Exploring for, and effectively exploiting geothermal resources are two of the most difficult challenges in energy development. Geothermal prospects typically occur in geologically complex environments, usually in volcanic or metamorphic terrains. Furthermore, they are complex physical systems with significant temperature, pressure, and chemical variations, often accompanied by fluid phase changes, and tectonically active with faulting and conductive fractures. The extreme heterogeneity and rugged topography that are often encountered in geothermal areas can render seismic reflection methods ineffective. The harsh sub-surface conditions, with high temperatures and corrosive fluids, severely limit or preclude well logging. Furthermore, the financial resources available for geothermal exploration are often much less than for hydrocarbon exploitation. As a result, passive techniques, such as heat-flow studies and micro-seismic monitoring are some of the most common methods used in geothermal exploration. However, these methods have several drawbacks. Heat flow observations are

point measurements and lack both spatial and temporal resolution. Micro-seismic methods are limited to areas were earthquakes occur, are indirectly related to the temperature and fluid pressure, and have a temporal sampling that depends upon the frequency of seismic events.

In this paper we discuss geodetic techniques for identifying and characterizing geothermal resources. These are methods for measuring the deformation of the Earth through various means. The technology for making such measurements has advanced considerably in the past few decades, with the development of downhole tilt meters, Global navigational satellite systems (GNSS), Interferometric Synthetic Aperture Radar (InSAR), and Light Detection and Ranging (LiDAR). Some advantages of these systems include cost-effectiveness, favorable temporal sampling from days to weeks for InSAR to seconds or minutes for tilt meters and GNSS receivers, almost continuous spatial coverage for InSAR and LiDAR, and often sub-centimeter precision. Furthermore, geodetic observations are one of the few remotely gathered data sets that have sensitivity to both effective pressure and temperature changes in the sub-surface. We will discuss the available geodetic methods and how they have been used to study geothermal systems. We conclude the paper with an illustration of the use of geodetic techniques to improve our understanding of The Geysers in California, currently the world's largest geothermal energy producing field.

Commonly Available Geodetic Methods

We provide a brief discussion of each of the geodetic techniques that are most commonly applied in geophysical exploration and monitoring. Due to its economic importance and its relationship to astronomy, geodesy has a long history and occupied major scientific figures, including Gauss. The early development of many geodetic techniques in the Earth sciences was for the study of natural hazards such as volcanoes (Dzurisin 2007) and earthquakes with their correspondingly larger ground deformation than that due to geothermal activity. However, several techniques have been adopted to study such processes as subsidence due to groundwater withdrawal (Vasco et al. 2019), ground movement induced by the sequestration of carbon dioxide (Vasco et al. 2020), deformation due to oil and gas development (Fielding et al. 1998), as well as to study surface displacements associated with geothermal production. LiDAR (Eitel et al. 2016), is one emerging technology that we shall not discuss. Although it has been used to map topography at potential geothermal sites in the state of Oregon, to our knowledge it has not yet been applied to the imaging of surface deformation at an existing geothermal field.

Leveling

Observations of vertical displacements obtained from leveling surveys are one of the oldest sources of geodetic data, along with triangulation measurements discussed below. In principle the technology is simple, a calibrated graduated staff or stadia rod is situated at a fixed distance from the observation point. In optical leveling a precision telescope is used to determine the vertical distance to the base of the rod relative to a horizontal line of sight. The local horizontal plane at the measurement point is defined with respect to the gravity vector using a bubble level. As might be imagined, such a definition of the horizontal plane ties leveling to the local gravity field in a given area. In order to maintain high accuracy, the process can require a number of corrections and quality control procedures that are well documented. One of the chief sources of error is the refraction of light between the observation point and the stadia rod due to temperature gradients near the ground surface.

Leveling is one of the first geodetic methods utilized at both potential and existing geothermal fields, often due to issues related to subsidence and damage to surface structures. It is typically conducted on roadways traversing a geothermal area and thus not generally applicable in undeveloped regions. For this reason, it has been largely supplanted by geodetic observations based upon Global Navigational Satellite Systems in many fields. Leveling is still a very common technique for measuring surface deformation and provides an important link with earlier deformation studies. Thus, it is particularly useful in areas with a long history, such as Yellowstone (Reilinger et al. 1977, Pelton and Smith, 1982, Vasco et al. 2007), Long Valley caldera (Castle et al. 1984, Vasco et al. 1988), and The Geysers in California (Lofgren 1981, Mossop and Segall 1997), but the approach has been used in many other fields such as the Okuaizu field in Japan (Vasco et al. 2002a, see Figure 1), the Leyte geothermal field in the Philippines (Apuada and Olivar, 2005), and the Cerro Prieto field in Mexico (Glowacka et al. 1999). In addition, as a ground-based technique, leveling observations avoid much of the atmospheric variability that impacts remote-sensing methods, although one must still contend with the issue of light refraction.

Triangulation and Trilateration

Triangulation involves accurately measuring the distance between two points and then using two angular observations to determine the geographic location of a third point that completes the triangle. It is a classic technique in geodesy that often takes advantage of unobstructed views from hills and mountain tops. Due to the advent of laser ranging and electronic distance measuring (EDM) techniques, triangulation has largely been supplanted by trilateration, whereby the lengths of the three sides of a triangle are measured with great accuracy. The technology was improved by the use of multiple wavelengths, allowing for corrections for atmospheric effects. Trilateration is most useful in rugged areas with well separated topographic high points for sighting, such as in northern California, an area containing The Geysers geothermal field (Prescott and Yu 1986). Other notable efforts were conducted in volcanic regions with considerable deformation including the

Yellowstone (Smith et al. 1989) and Long Valley (Langbein 1989) calderas. Due to its sparse distribution and large spatial averaging (Figure 2), trilateration measurements are often used in conjunction with other types of geodetic observations, such as leveling data, in order to constrain source models of geothermal features. Such approaches have been applied at both Long Valley in California (Battaglia and Vasco 2006) and at the Yellowstone caldera.

Tilt

Tilt is another geodetic technique with a rather long history. The earliest method utilized a long-length stationary pendulum but these instruments lacked portability. Currently, the most common approaches rely on the fact that the surface of a fluid remains normal to the direction of gravity, the principle of the bubble level. This approach has been implemented in pipes containing fluid to increase sensitivity while maintaining portability (Eaton 1959) and, more compactly, using a conducting fluid such a mercury and resistivity changes to sense minute changes in the bubble position (Westphal et al. 1983). Due to daily thermal effects and Earth tides, most accurate tilt measurements are made in boreholes, generally ten or more meters in depth (Wright 1998). Permanent down hole sensors have a self-leveling capability in order to increase their range to larger tilts. Newer approaches based upon micro-electromechanical (MEM) sensors, including miniaturized accelerometers, are under development, potentially leading to smaller instruments. These MEM sensors can be precisely calibrated, improving both accuracy and stability. Two characteristics of down hole tilt measurements are: favorable temporal sampling, with observations every minute, and isolation from the surface, a real advantage in area subject to snow cover and vegetation changes.

Tilt has been used to for monitoring at a limited number of geothermal fields, including Long Valley, California, Wairakei, New Zealand, and the Hijiori and Okuaizu sites in Japan (Mortensen and Hopkins 1987, Bibby and Hurst 1990, Vasco et al. 2002a). While tilt meters have been used in the oil industry for monitoring short term operations, in particular to characterize hydro-fracture development (Wright 1998), there have been few such efforts in geothermal fields. In Vasco et al. (2002a) an injection into a roughly 2 km deep borehole was monitored using a network of 20 borehole tilt meters. While the injection occurred during the day, the most significant tilt was observed at night, in the hours following the injection. Furthermore, the tilt vectors did not form a simple pattern indicating uniform flow away from the well (Figure 3). Rather, the pattern of tilt vectors suggests complicated flow in response to a heterogeneous permeability distribution. In fact, an inversion of the tilt data for volume changes at depth indicates fluid migration along ring fractures of the volcanic structure (Figure 3), with some of the largest volume changes at fracture intersections. Similar migration along fractures were observed during an experiment at the Okuaizu geothermal field at which a network of 14 tilt meters were used to monitor the start-up of injection and production in the field after a month of maintenance (Vasco et al. 2002a).

The tilt evolution for over 30 days following the start-up indicated flow along known fractures in the field, plotted in Figure 1, and again suggested preferential flow at fracture intersections.

Global Navigational Satellite Systems

Global Navigational Satellite Systems (GNSS), of which the Global Positioning System (GPS) is probably the most well-known example, provide a form of dynamic, three-dimensional trilateration (Dixon 1991, Teunissen and Kleusberg 1998, Hofmann-Wellenhof et al. 2007). That is, a network of closely tracked satellites send signals to receivers on the Earth's surface and the signals are post-processed to get accurate arrival times for triangulation. There are several sources of error that must be corrected for including atmospheric effects, multipathing, clock drift, and satellite location errors among other factors. Due to the processing requirements, GPS data are not available in real time and require sophisticated software for the extraction of the three components of the displacement vector. Differential GNSS estimates of displacements relative to a base station are the most accurate, as this reduces the errors from several sources. However, as with electronic distance measurements and laser ranging, the use of dual-frequency instruments helps to estimate and to correct for the effect of the atmosphere, resulting in relative location errors of the order of 1 to 3 centimeters. Key advantages of satellite-based location systems like GPS are almost continuous temporal resolution and the availability of all three components of the displacement vector. Global satellite systems such as GPS have seen extensive applications in the Earth sciences since their development in the 1980's (Bürgmann and Thatcher 2013, Bock and Melgar 2016). As with geodetic methods in general, the earliest applications were to tectonically active areas that posed potential hazards and large deformation, such as fault systems and volcanic features. Specific applications to hydrothermal and geothermal fields followed, most significantly in areas with large volcanic-related features such as The Geysers in California (Mossop and Segall 1997, Floyd and Funning 2013), Yellowstone (Smith et al. 1989) and Long Valley calderas (Webb et al. 1995), and the Reykjanes peninsula in Iceland (Hreinsdottir et al. 2001). The disadvantages of using GNSS are the expense of deploying the receivers and the fact that these are point measurements. Regional GNSS networks provide stable long-term vector displacement data for the imaging of tectonic strain that is critical for many applications, such as the monitoring for natural hazards.

The stability of GNSS, and its capabilities for the long-term imaging of strain, has proven to be valuable in exploring for new geothermal fields. The motivation for associating actively deforming areas with geothermal prospects is rooted in the observation by Blewitt et al. (2003) of a correspondence between high geothermal temperatures and crustal strain in Nevada's Great Basin over length scales of 10's to 100's of kilometers, as measured by GPS observations (Figure 4). This observation, coupled with data on the age of recent faulting, slip

rates on recent faults, slip and dilatation on Quaternary faults, earthquake density, gravity gradients, geochemistry from subsurface fluids, and temperature gradients from boreholes, has led to a play fairway analyses of the geothermal potential of Nevada's Great Basin (Faulds et al. 2018) and Washington state (Swyer et al. 2018). Play fairway analysis, developed in the oil industry (Doust 2010), utilizes the geological and geophysical data to determine the probability of an economic resource at a given location. In particular, sets of observations are combined to give a score indicating the likelihood of an exploitable geothermal field. As an example, Figure 5 displays the contribution of the permeability component of the play fairway score for a large area of the Great Basin. In order to compute the score, the horizontal gravity gradient was multiplied by 1.7, the geodetic strain by 1.5 and the earthquake density by 1.0 (Faulds et al. 2018). There appears to be a good correspondence between a high play fairway score and the location of geothermal systems.

Interferometric Synthetic Aperture Radar

Interferometric Synthetic Aperture Radar (InSAR) has become the geodetic method of choice for monitoring deformation associated with geothermal production. In fact, some of the earliest applications of InSAR were observations related to subsidence due to geothermal production (Massonnet et al. 1997, Carnec and Fabriol 1999). The characteristics that contribute to its appeal for monitoring geothermal fields are the fact that it is a remote sensing technique, usually satellite-based, and requiring no expensive field campaigns, it samples areas with high spatial resolution, and satellite revisit times are months to weeks. The data are widely available from several governmental agencies around the world. A particularly useful collection of observations is provided by the Sentinel satellite constellation, operated by the European Space Agency. These data are available to research institutions for a nominal fee or at no cost. While the technology and processing associated with estimates of surface deformation are sophisticated (Gabriel et al. 1989, Massonnet and Feigl 1998, Bürgmann and Thatcher 2013, Ferretti 2014), the underlying principle is similar to that of echo location (Figure 6).

A microwave chirp from an orbiting satellite propagates to the Earth's surface where it is reflected from various scattering points and the return is stored for later use. Several stages of processing result in very accurate estimates of changes in the effective signal phase for points on the surface of the Earth (Ferretti 2014). The interferograms are then mapped into range change, the movement of the object in the line-of-sight direction (Figure 6). As might be imagined, changes in the characteristics of the Earth's surface between satellite passes can have a pronounced effect on the estimates of range change. Extensive vegetation, snow cover, and wind-blown sand are some of the more common issues, particularly for the shorter wavelength C-band InSAR data. However, processing technology has advanced and improved satellite hardware and orbital configurations, including shortened return time of 6 days, have helped to overcome or mitigate many of these problems (Lanari et al. 2004, Hooper 2008, Ferretti et al. 2011, Samsonov and d'Oreye 2012). As a last resort, surface reflectors

may be installed, but this eliminates some of the inherent advantages of InSAR monitoring (Ferretti 2014). An up-to-date overview of radar interferometry by Ming et al. (2020) covers the many approaches that we do not have the space to include in this short discussion.

There are far too many studies that use SAR interferometry to characterize the deformation of geothermal fields for us to review and list in this short article. Thus, out of necessity, we only cite a few of the numerous published studies and form some general conclusions on the current state of InSAR analysis at geothermal fields. As noted above, InSAR performs well in the absence of snow and vegetation and studies of geothermal fields in deserts and areas with bare and rocky ground were the most successful with the early C-band InSAR satellite configurations from the 1990's until sometime after 2010. Thus, several studies followed those of Massonnet et al. (1997) and Carnec and Fabriol (1999) and focused on fields in the Imperial Valley of California, including the Salton Sea, Heber, and East Mesa geothermal fields (Eneva et al. 2012, Barbour et al. 2016), and on the Cerro Prieto field in Mexico (Sarychikhina et al. 2018). The Coso geothermal field, also in the California desert, provided another favorable site for the early application of InSAR (Fialko and Simons 2000, Wicks et al. 2001, Vasco et al. 2002a). Several geothermal fields are also found in the sparsely-vegetated basin and range of western North America and InSAR has been used to study the Brady's (Reinisch et al. 2018) and San Emidio geothermal fields among others (Oppliger et al. 2005, Ali et al. 2016). The Geysers geothermal field was also an early target for the application of InSAR, but initially it proved too difficult. It was not until techniques such as the permanent scatterer approach were developed, and satellites with shorter return times were available, before InSAR was successful at The Geysers (Vasco et al. 2013). Other sites in the US include Raft River (Liu et al. 2018) and Hawaii. Monitored geothermal sites outside of the US include fields in Iceland (Keiding et al. 2010, Juncu et al. 2020), New Zealand (Hole et al. 2007), Africa, and Central and South America.

The inversion methods for developing source models to explain the InSAR observations are evolving along with the technology, albeit slowly. It is still common practice to use the InSAR data to determine some set of point pressure or volume source models (Barbour et al. 2016, Juncu et al. 2020), rectangular dislocation Okada (1985) models, pressurized ellipsoidal bodies (Fialko and Simons 2000), or polygonal bodies (Opplinger et al. 2005). Such prescribed models are likely to introduce biases into the inversion procedure. It is possible to construct more elaborate distributed source models to represent general heterogeneous volume changes associated with geothermal production and injection (Vasco et al. 1988, Mossop and Segall 1999). For example, Vasco et al. (2002b) developed a spatially-varying, three-layer, volume change model of the Coso geothermal reservoir undergoing contraction due to fluid pressure reduction and temperature changes (Figure 7). Even today, such model building is not that common in the interpretation of InSAR observations from geothermal fields, perhaps due to the loss of resolution with depth that is associated with geodetic data gathered at the Earth's surface

(Mossop and Segall 1999, Vasco et al. 2002b). A related issue of the non-uniqueness inherent in such inversions, whereby multiple solutions can fit the same data set. Such non-uniqueness is particularly acute in models containing multiple layers due to trade-offs in anomalies at different depths.

The resolution issue points to the need for physically meaningful regularization to constrain the range of possible solutions. In the case of deformation related to fluid injection and production, it is possible to use the locations of the active wells to devise a distance penalty term to favor solutions with volume changes around the wells (Vasco et al. 2019). Such a distance constraint is also possible in the case of seismic activity related to cool fluid inducing contraction and stresses in a region around the well, a common occurrence at The Geysers geothermal field. If the injected and produced fluid volumes are known, one can use the fractional fluid volume changes to derive a prior model and constrain the solution to honor these volume changes if it is possible to do so while still fitting the data (Vasco et al. 2017). This approach must be modified in a geothermal field in order to account for effects such as thermoelastic volume changes due to differences in the temperatures between the fluids and the host rock, as well as variations in poroelastic and multi-phase properties within the reservoir (Juncu et al. 2019).

Another limitation of most current modeling efforts is the use of a homogeneous half-space as the elastic structure of the geothermal field. As noted above, geothermal fields are often highly heterogeneous volcanic regions and almost certainly deviate from a homogeneous medium. It has been noted how observed surface deformation is impacted by any spatial variations in the elastic properties surrounding a source (Vasco et al. 2010). Fully three-dimensional poroelastic structures can produce detailed changes in the spatial variations in the stress field and significant deviations in the stress magnitudes from those of a homogeneous medium (Vasco et al. 2017). A more comprehensive modeling and inversion approach relies on a coupled reservoir simulator to relate the injected and produced fluid volumes to the surface deformation. Although there are adjoint formulations for the coupled hydrological-mechanical inversion problem (Iglesias and McLaughlin 2012, Hesse and Stadler 2014), the methods estimate flow properties, such as permeability, and not the source distribution itself. To date, source models derived using coupled simulation have relied on trial and error model adjustments, due to the long simulation times required for one forward run (Liu et al. 2018). Future improvements are likely to overcome these limitations.

Geodetic Studies at The Geysers Geothermal Field in California

The Geysers is the largest geothermal producing field in the world and has a long operational history. It is in a tectonically active area in northern California (Figure 8), and has been the subject of several of geodetic field campaigns and studies. Due to its rugged topography it has been a difficult location for field work. The Geysers

site has become a major source of seismicity in northern California and has been actively deforming, both from the regional tectonics and the geothermal production. The first geodetic measurements were leveling surveys conducted in the 1970's by the US Geological Survey along roads traversing the region (Lofgren 1981). An average subsidence rate of 4.8 cm/year was estimated from the observations between 1973 and 1977. Following the development of the satellite-based Global Positioning System, it was used in The Geysers in the mid-1990's to further characterize the on-going deformation (Mossop and Segall (1997, 1999). These campaign-style GPS surveys were followed by additional surveys in 2006, 2009, 2010, and 2011 (Floyd and Funning 2013). The surveys were conducted after the completion of two water injection pipelines, the Southeast Geysers Effluent Pipeline and the Santa Rosa Geysers Recharge Pipeline, that were constructed in order to sustain reservoir steam pressure at The Geysers to maintain its long-term viability. In conjunction with those campaigns, two continuous GPS instruments were installed for long term monitoring, with the goal of installing network of permanent stations. The rate of subsidence was found to decrease following the operation of the two pipeline projects (Floyd and Funning 2013). A trilateration network was also operated in northern California, primarily to monitor the San Andreas fault system but it did provide coverage of a portion of The Geysers (Prescott and Yu 1986). The network observations indicated a decrease in the rate of deformation across the Geysers, a deviation from the expected linearity, after 1978. Mossop and Segall (1999) conducted an inversion of the leveling and GPS data for grid block volume changes on a four-layer regular grid. Because the inversion did not constrain the depth of the volume change nor restrict the volume change to be within the reservoir interval, the inversion put the majority of the volume change in the top layer of the model, between 0 and 1 km in depth. Still, Mossop and Segall (1999) noted a spatial correlation between the estimated volume changes on the grid between 1977 and 1996, and the reservoir pressure observed in 1987. Furthermore, they found some correspondence between the volume changes and seismicity within the Geysers.

Early attempts to extract range change estimates from InSAR data at The Geysers were not successful. However, later work utilizing a permanent scatterer approach did produce reliable range changes from C-band data (Rutqvist 2011). Further work with the more frequently sampled X-band data and the enhanced approach of Ferretti et al. (2011) provided even denser spatial coverage (Vasco et al. 2013) and much better temporal resolution. In fact, the time series from the X-band observations allowed for the monitoring of a well test associated with the development of an enhanced geothermal system (EGS), along with seasonal variations due to groundwater variations and fluctuations in production and injection (Jeanne et al. 2014). Improvements in both satellite characteristics and processing techniques are continuing and it is now possible to image production-related deformation over most of The Geysers (Figure 9) and to determine quasi-vertical and quasi-

east-west components as in Samsonov and d'Oreye (2012). Furthermore, the temporal sampling has improved and satellite return times of as little as 6 days are possible.

Interpreting observed InSAR range change at The Geysers is complicated by a number of factors. The steep slopes in the area produce numerous landslides that obscure reservoir deformation. In addition, tectonic activity and faulting also produce ground deformation. There are a large number of operating wells and they can produce interfering ground motion. Fluid pressure, temperature, and phase changes can all strain the reservoir and deform the ground surface. Nonetheless, it is possible to use the InSAR observations to improve our understanding of flow in The Geysers. One particular fruitful approach is to combine InSAR data with seismicity. For example, a combination of observed deformation and seismicity were used to construct a three-dimensional hydrological/geomechanical model of the region around the EGS site, including a network of two sets of intersecting shear zones influencing flow between the wells: a low permeability zone trending to the northwest and a high permeability NW-striking zone (Jeanne et al. 2014, Rutqvist et al. 2016). The successful use of seismicity data, generated during injection at the EGS well, has motivated the field operator to conduct a field-wide analysis of the earthquake data for controlling faults in the field (Hartline et al. 2015, 2019). A combination of three-dimensional visualization and high-quality earthquake locations made it possible to identify lineations that define trends and bound seismicity.

A concerted effort to identify the important faults in The Geysers geothermal field resulted in a three-dimensional model of the fault distribution within the field (Figure 10). In order to determine the faults, the seismicity is rotated until surfaces are visible. Seismic events are selected in order to construct tessellated surfaces for the suspected faults (Hartline et al. 2019). The surfaces are refined as the field is produced and are part of an evolving three-dimensional structural model for The Geysers. The surfaces appear to have predictive power regarding the encounters of fault/fracture systems during the drilling of wells. Furthermore, a preliminary analysis of recent InSAR data from the Geysers indicates an element of fault control for flow related to geothermal production and injection. In particular, the range change observed above a pair of wells, just to the north of the EGS site at wells Prati-32 and Prati State-31, display a sharp transition from subsidence associated with a producer to uplift corresponding to an injector (Prati-9). While the data quality is marginal in this region and there are gaps in the estimates of range change, the linear nature of the boundary in Figure 11 is suggestive of a fault impeding flow between the wells. In addition, the linear edge is also the boundary of seismicity associated with injection into well Prati-9. More work is necessary to compare the seismicity and range change in other areas in The Geysers.

Conclusions

Due to large fluid fluxes that are associated with geothermal fields they often generate observable surface deformation, even when the reservoirs are several kilometers deep. Thus, geodetic data can be a valuable source of information on the flow within the field. In addition, strain measurement can be used to identify geothermal prospects based upon a play fairway analysis. While there have been numerous inversions of geodetic data at geothermal fields, the current practice of interpreting these observations could be improved. If at all possible, one should use a realistic three-dimensional structural model for the field under study. This is particularly important if micro-earthquakes are to be incorporated into the analysis because stress estimates are very sensitive to mechanical properties at depth. Due to the resolution issues associated with geodetic data gathered on the surface, a meaningful choice of the regularization is critical. Similarly, an integrated or joint inversion with other data sets could help reduce the non-uniqueness. A realistic source model or a flexible representation should be used in order to reduce the chance of biasing the solution. Coupled fluid flow and geomechanics simulators will provide the greatest fidelity. However, their use in an inversion algorithm will require additional advances in its formulation, as a single forward run might require days of computation.

References

Ali, S. T., Akerley, J., Baluyut, E. C., Cardiff, M., Davatzes, N. C., Feigl, K. L., Foxall, W., Fratta, D., Mellors, R. J., Spielman, P., Wang, H., and Zemach, E., 2016, Time-series analysis of surface deformation at Brady Hot Springs geothermal field (Nevada) using interferometric synthetic aperture radar, Geothermics, **61**, 114-120.

Apuada, N. A., and Olivar, R. E. R., 2005, Repeat microgravity and leveling surveys at Leyte geothermal production field, north central Leyte, Philippines, Proceeding World Geothermal Congress, Antalya, Turkey, April 2005.

Barbour, A. J., Evans, E. L., Hickman, S. H., and Eneva, M., 2016, Subsidence rates at the southern Salton Sea consistent with reservoir depletion, Journal of Geophysical Research, **121**, 5308-5327.

Battaglia, M., and Vasco, D. W., 2006, The search for magma reservoirs in Long Valley Caldera: single versus distributed sources, in Troise, C., De Natale, G, and Kilburn, C. R. J. (eds.) Mechanisms of Activity and Unrest at Large Calderas, Geological Society, London, Special Publications, **269**, 173-180.

Bibby, H. M., and Hurst, A. W., 1990, Tilt monitoring at Wairakei geothermal field, Geothermics, **19**, 385-396.

Blewitt, G., Coolbaugh, M., Holt, W., Davis, J., and Bennett, 2003, Targeting of potential geothermal resources in the Great Basin from regional- to basin-scale relationships between geodetic strain and geologic structures, Geothermal Resources Council Transactions, **27**, 3-7.

Blewitt, G., Hammond, W. C., and Kreemer, C., 2005, Relating geothermal resources to Great Basin tectonics using GPS, Geothermal Resources Council Transactions, **29**, 331-336.

Bock, Y. and Melgar, D., 2016, Physical applications of GPS geodesy: a review. *Reports on Progress in Physics*, **79**, 10, 106801.

Bürgmann, R., and Thatcher, W., 2013, Space geodesy: A revolution in crustal deformation measurements of tectonic processes. *Geological Society of America, Special Paper* **500.**

Carnec, C., and Fabriol, H., 1999, Monitoring and modeling land subsidence at the Cerro Prieto geothermal field, Baja California, Mexico, using SAR interferometry, Geophysical Research Letters, **26**, 1211-1214.

Castle, R. O., Estrem, J. E., and Savage, J. C., 1984, Uplift across Long Valley caldera, California, Journal of Geophysical Research, **89**, 11507-11515.

Dixon, T. H., 1991, An introduction to the Global Positioning System and some geological applications, *Reviews of Geophysics*, **29**, 249-276.

Doust, H., 2010, The exploration play: what do we mean by it? American Association of Petroleum Geologists Bulletin, **94**, 1657-1672.

Dzurisin, D., 2007, Volcano Deformation-Geodetic Monitoring Techniques, Springer, Chichester, UK.

Eaton, J. P., 1959, A portable water-tube tiltmeter, Bulletin of the Seismological Society of America, **49**, 301-316.

Eitel, J. U. H., Hofle, B., Vierling, L. A., Abellan, A., Asner, G. P., Deems, J. S., Glennie, C. L., Joerg, P. C., Lewinter, A. L., Magney, T. S., Mandlburger G., Morton, D. C., Muller, J., and Vierling, K. T., 2016, Beyond 3-D: The new spectrum of LiDAR applications for Earth and ecological sciences, *Remote Sensing of Environment*, **186**, 372-392.

Eneva, M., Adams, D., Falorni, G., and Morgan, J., 2012, Surface deformation in Imperial Valley, CA, from satellite radar interferometry, Geothermal Research Council Transactions, **36**, 1339-1344.

Faulds, J. E., Craig, J. W., Coolbaugh, M. F., Hinz, N. H., Glen, J. M., and Deoreo, S., 2018, Search for blind geothermal systems utilizing Play Fairway Analysis, western Nevada, Geothermal Resources Council Bulletin, **47**, 34-42

Fialko, Y. and Simons, M., 2000, Deformation and seismicity in the Coso geothermal area, Inyo County, California: Observations and modeling using satellite radar interferometry, Journal of Geophysical Research, **105**, 21781-21794.

Ferretti, A., 2014, *Satellite InSAR Data – Reservoir Monitoring from Space*. EAGE Publications.

Ferretti, A., Fumagalli, A., Novali, F., Prati, C, Rocca, F., and Rucci, A., 2011, A new algorithm for processing interferometric data-stacks: SqueeSAR, IEEE Transactions on Geoscience and Remote Sensing, **49**, 3460-3470.

Fielding, E. J., Blom, R. G., and Goldstein, R. M., 1998, Rapid subsidence over oil fields measured by SAR interferometry, Geophysical Research Letters, **25**, 3215-3218.

Floyd, M. A., and Funning, G. J., 2013, Continuation of survey GPS measurements and installation of continuous GPS sites at The Geysers, California, for geothermal deformation monitoring, Geothermal Research Council Transactions, **37**, 895-898

Gabriel, A. K, Goldstein, R. M., and Zebker, H. A., 1989, Mapping small elevation changes over large areas: Differential radar interferometry, Journal of Geophysical Research, **94**, 9183-9191.

Geertsma, J., 1973, Land subsidence above compacting oil and gas reservoirs, Journal of Petroleum Technology, **25**, 734-744

Glowacka, E., Gonzalez, J., and Fabriol, H., 1999, Recent vertical deformation in Mexicali Valley and its relationship with tectonics, seismicity, and the exploitation of the Cerro Prieto geothermal field, Mexico, Pure and Applied Geophysics, **156**, 591-614.

Hartline, C. S., Walters, M. A., and Wright, M. C., 2015, Three-dimensional structural modeling building, induced seismicity analysis, drilling analysis, and reservoir management at The Geysers Geothermal field, northern California, Geothermal Resources Council Transactions, **39**, 603-614.

Hartline, C. S., Walters, M. A., and Wright, M. C., 2019, Three-dimensional structural model building constrained by induced seismicity alignments at The Geysers Geothermal field, northern California Geothermal Resources Council Transactions, **43**, 1-24.

Hesse, M. A., and Stadler, G., 2014, Joint inversion in coupled quasi-static poroelasticity, Journal of Geophysical Research, 119, 1425-1445.

Hofmann-Wellenhof, B., Lichtenegger, H. and Wasle, E., 2007, *GNSS-Global Navigation Satellite Systems: GPS, GLONASS, Galileo, and More* (Wien: Springer).

Hole, J. K., C. J. Bromley, N. F. Stevens, and G. Wadge, 2007, Subsidence in the geothermal fields of the Taupo Volcanic Zone, New Zealand from 1996 to 2005 measured by InSAR, Journal of Volcanology and Geothermal Research, 166, 125-146.

Hooper, A., 2008, A multi-temporal InSAR method incorporating both persistent scatterer and small baseline approaches, *Geophysical Research Letters***, 35**, L16302, 1-5.

Hreinsdottir, S., and Einarsson, P., and Sigmundsson, Freysteinn, 2001, Crustal deformation at the oblique spreading Reykjanes Penisula, SW Iceland: GPS measurements from 1993 to 1998, Journal of Geophysical Research**, 106**, 13803-13816.

Iglesias, M. A., and McLaughlin, D., 2012, Data inversion in coupled sub-surface flow and geomechanics, Inverse Problems, **28**.

Jeanne, P., Rutqvist, J., Vasco, D., Garcia, J., Dobson, P. F., Walters, M., Hartline, C., and Borgia, A., 2014, A 3D hydrological and geomechanical model of an Enhanced Geothermal System at The Geysers, California, Geothermics, **51**, 240-252.

Juncu, D., Arnadottir, T., Geirsson, H., Gudmundsson, G. B., Lund, B., Gunnarsson, G., Hooper, A., Hreinsdottir, S., and Michalczewska, K., 2020, Injection-induced surface deformation and seismicity at the Hellisheidi geothermal field, Iceland, Journal of Volcanology and Geothermal Research, **391**, 1-13.

Juncu, D., Arnadottir, Th., Geirsson, H., and Gunnarsson, G., 2019, The effects of fluid compressibility and elastic properties on deformation of geothermal reservoirs, Geophysical Journal International, 217, 122-134.

Keiding, M., T. rnadottir, S. Jonsson, J. Decriem, and A. Hooper (2010), Plate boundary deformation and man-made subsidence around geothermal fields on the Reykjanes Peninsula, Iceland, Journal of Volcanology and Geothermal Research, **194**, 139-149

Langbein, J., 1989, Deformation of the Long Valley caldera, eastern California, from mid-1983 to mid-1988: Measurements using a two-color geodimeter, Journal of Geophysical Research, **94**, 3833-3849.

Lanari, R., Mora, O., Manunta, M., Mallorqui, J. J., Berardino, P, and Sansosti, E., 2004, A small baseline approach for investigating deformations on full-resolution differential SAR interferograms, *IEEE Transactions on Geoscience and Remote Sensing*, **42**, 1377-1386.

Lofgren, B. E., 1981, Monitoring crustal deformation in the Geysers-Clear Lake region. In Research in The Geysers-Clear Lake geothermal area, North California. U. S. Geological Survey Professional Paper **1141**, US Government Printing Office.

Liu, F., Fu, P., Mellors, R. J., Plummer, M. A., Ali, S. T., Reinisch, E. C., Liu, Q., and Feigl, K. L., 2018, Inferring geothermal reservoir processes at the Raft River Geothermal Field, Idaho, USA, Through modeling InSAR-measured surface deformation, Journal of Geophysical Research, **123**, 3645-3666.

Massonnet, D., and Feigl, K., 1998, Radar interferometry and its application to changes in the Earth's surface, Reviews of Geophysics, **36**, 441-500.

Massonnet, D., Holzer, T., and Vadon, H., 1997, 1997, Land subsidence caused by the East Mesa geothermal field, California, observed using SAR interferometry, Geophysical Research Letters, **24**, 901-904.

Ming, D. H. T., Hanssen, R., and Rocca, F., 2020, Radar interferometry: 20 years of development in time series techniques and future perspectives, Remote Sensing, **12**, 1-18, doi: 10.3390/rs12091364.

Mortensen, C. E., and Hopkins, D. G., 1987, Tiltmeter measurements in Long Valley caldera, California, Journal of Geophysical Research, **92**, 13767-13776.

Mossop, A., and Segall, P., 1997, Subsidence at The Geysers geothermal field, N. California from a comparison of GPS and leveling surveys, Geophysical Research Letters, **24**, 1839-1842.

Mossop, A., and Segall, P., 1999, Volume strain within The Geysers geothermal field, Journal of Geophysical Research, **104**, 29113-29131.

Okada, Y., 1992, Internal deformation due to shear and tensile faults in a half-space, Bulletin of the Seismological Society of America, **82**, 1018-1040.

Oppliger, G., Coolbaugh, M., Shevenell, L., and Taranik, J., 2005, Elucidating deep reservoir geometry and lateral outflow through 3-D elastostatic modeling of satellite radar (InSAR) observed surface deformation: An example from the Bradys geothermal field, Geothermal Resources Council Transactions, **29**, 419-424.

Pelton, J. R., and Smith, R. B., 1982, Contemporary vertical surface displacements in Yellowstone National Park, Journal of Geophysical Research, **87**, 2745-2761.

Prescott, W. H., and Yu, S.-B., 1986, Geodetic measurements of horizontal deformation in the northern San Francisco Bay region, California, Journal of Geophysical Research, **91**, 7475-7484.

Reilinger, R. E., Citron, G. P. and Brown, L. D., 1977, Recent vertical crustal movements from precise leveling data in southwestern Montana, western Yellowstone National Park, and the Snake River Plain, Journal of

Geophysical Research, **82**, 5349-5359.

Reinisch, E. C., Cardiff, M. and Feigl, K. L., 2018, Characterizing Volumetric Strain at Brady Hot Springs, Nevada, USA Using Geodetic Data, Numerical Models, and Prior Information, Geophysical Journal International, **215**, 1501-1513.

Rutqvist, J., 2011, Status of the TOUGH-FLAC simulator and recent applications related to coupled fluid flow and crustal deformation, Computers in Geosciences, **37**, 739-750.

Rutqvist, J., Jeanne, P., Dobson, P. F., Garcia, J. Hartline, C., Hutchings, L., Singh, A., Vasco, D. W., and Walters, M., 2016, The northwest Geysers EGS demonstration project, California-Part 2: Modeling and interpretation, Geothermics, **63**, 120-138.

Samsonov, S., d'Oreye, N., 2012, Multidimensional time series analysis of ground deformation from multiple InSAR data sets applied to Virunga Volcanic Province. Geophysical Journal International, **191**, 1095-1108, http://dx.doi.org/10.1111/j.1365-246X.2012.05669.x.

Sarychikhina, O., Glowacka, E., and Robles, B., 2018, Multi-sensor DInSAR applied to the spatiotemporal evolution analysis of ground surface deformation in Cerro Prieto basin, Baja, California, Mexico, for the 1993-2014 period, Natural Hazards, **92**, 225-255.

Smith, R. B, Reilinger, R. E., Meertens, C. M., Hollis, J. R., Holdahl, S. R., Dzurisin, D., Gross, W. K., and Klingele, E. E., 1989, What's moving at Yellowstone?, EOS, **70**, 113-125.

Swyer, M. W., Cladouhos, T. T., Forson, C., Steely, A. N., and Davatzes, N. C., 2018, Simulating local sources of crustal deformation for Washington State geothermal prospects using geomechanical models, Abstract 18-464, American Rock Mechanics Association Symposium, Seattle, Washington, 17-20 June 2018, 1-9.

Teunissen P J, and Kleusberg, A., 1998, *GPS for Geodesy* (Berlin: Springer)

Vasco, D. W., Johnson, L. R., and Goldstein, N. E., 1988, Using surface displacement and strain observations to determine deformation at depth, with an application to Long Valley caldera, California, Journal of Geophysical Research, **93**, 3232-3242.

Vasco, D. W., Karasaki, K., and Nakagome, O., 2002a, Monitoring production using surface deformation: the Hijiori test site and the Okuaizu geothermal field, Japan, Geothermics, **31**, 303-342.

Vasco, D. W., Wicks, C., Karasaki, K., and Marques, O., 2002b, Geodetic imaging: reservoir monitoring using satellite interferometry, Geophysical Journal International, **149**, 555-571.

Vasco, D. W., Puskas, C. M., Smith, R. B., and Meertens, C. M., 2007, Crustal deformation and source models of the Yellowstone volcanic field from geodetic data, Journal of Geophysical Research, **112**, 1-19.

Vasco, D. W., Rucci, A., Ferretti, A., Novali, F., Bissell, R. C., Ringrose, P. S., Mathieson, A. S., and Wright, I. W., 2010, Satellite-based measurements of surface deformation reveal fluid flow associated with the geological storage of carbon dioxide, Geophysical Research Letters, **37**, 1-5.

Vasco, D. W., Rutqvist, J., Ferretti, A., Rucci, A., Bellotti, F., Dobson, P., Oldenburg, C., Garcia, J., Walters, M., and Hartline, C., 2013, Monitoring deformation at the Geysers Geothermal Field, California, using C-band and X-band interferometric synthetic aperture radar, Geophysical Research Letters, **40**, 1-6.

Vasco, D. W., Harness, P., Pride, S., and Hoversten, M., 2017, Estimating fluid-induced stress change from observed deformation, Geophysical Journal International, **208**, 1623-1642.

Vasco, D. W., Farr, T. G., Jeanne, P., Doughty, C., and Nico, P., 2019, Satellite-based monitoring of groundwater depletion in California's Central Valley, *Nature Scientific Reports*, **9**, 16043, doi.org/10.1038/s41598-019-52371-7.

Vasco, D. W., Dixon, T. H., Ferretti, A. and Samsonov S. V., 2020, Monitoring the fate of injected CO2 using geodetic techniques, *The Leading Edge*, January, 29-37.

Webb, F. H., Bursik, M., Dixon, T., Farina, F., Marshall, G., and Stein, R. S., 1995, Inflation of Long Valley Caldera from one year of continuous GPS observations, Geophysical Research Letters, **22**, 195-198.

Westphal, J. A., Carr, M. A., Miller, W. F., and Dzurisin, D., 1983, Expendable bubble tiltmeter for geophysical monitoring, Review of Scientific Instruments, **54**, 415-418.

Wicks, C. W., Thatcher, W., Monastero, F. C., and Hasting, M. A., 2001, Steady state deformation of the Coso Range, east central California, inferred from satellite radar interferometry, Journal of Geophysical Research, **106**, 13769-13780.

Wright, C. A., 1998, Tiltmeter fracture mapping: From the surface and now downhole, Petroleum Eng. Int., **71**, 50-63.

Xu, X., Sandwell, D. T., Tymofyeyeva, E., Gonzalez-Ortega, A., and Tong, X., 2017, Tectonic and Anthropogenic Deformation at the Cerro Prieto Geothermal Step-Over Revealed by Sentinel-1A InSAR, IEEE Transactions on Geoscience and Remote Sensing, **55**, 5284-5292

Figures

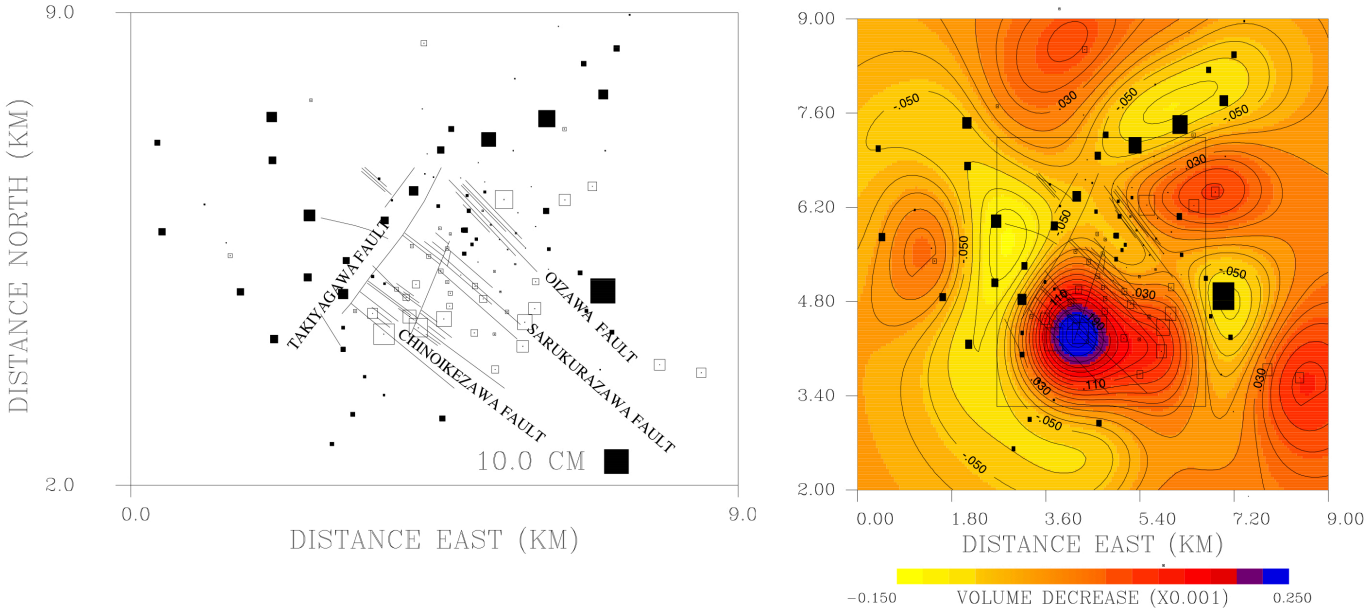

Figure 1. (Left) Leveling data gathered at the Okuaizu geothermal field in Japan. (Right) Volume change within the reservoir estimated from the leveling data (From Vasco et al. 2002a).

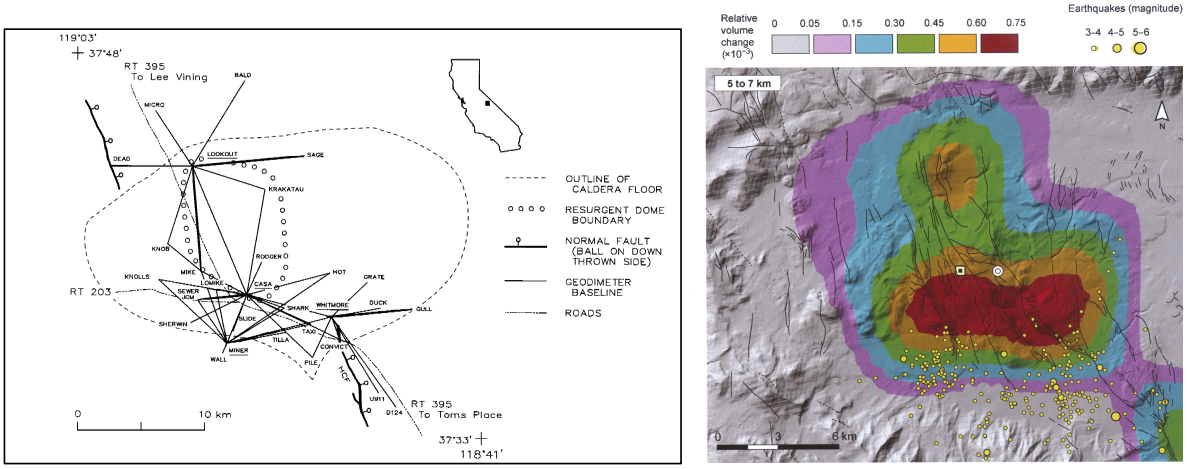

Figure 2. (Left) Trilateration network at Long Valley caldera, California (from Langbein 1989). The solid lines are sight-lines between stations. (Right) Volume change source model obtained by an inversion of trilateration, leveling, and GPS data (from Battaglia and Vasco 2006).

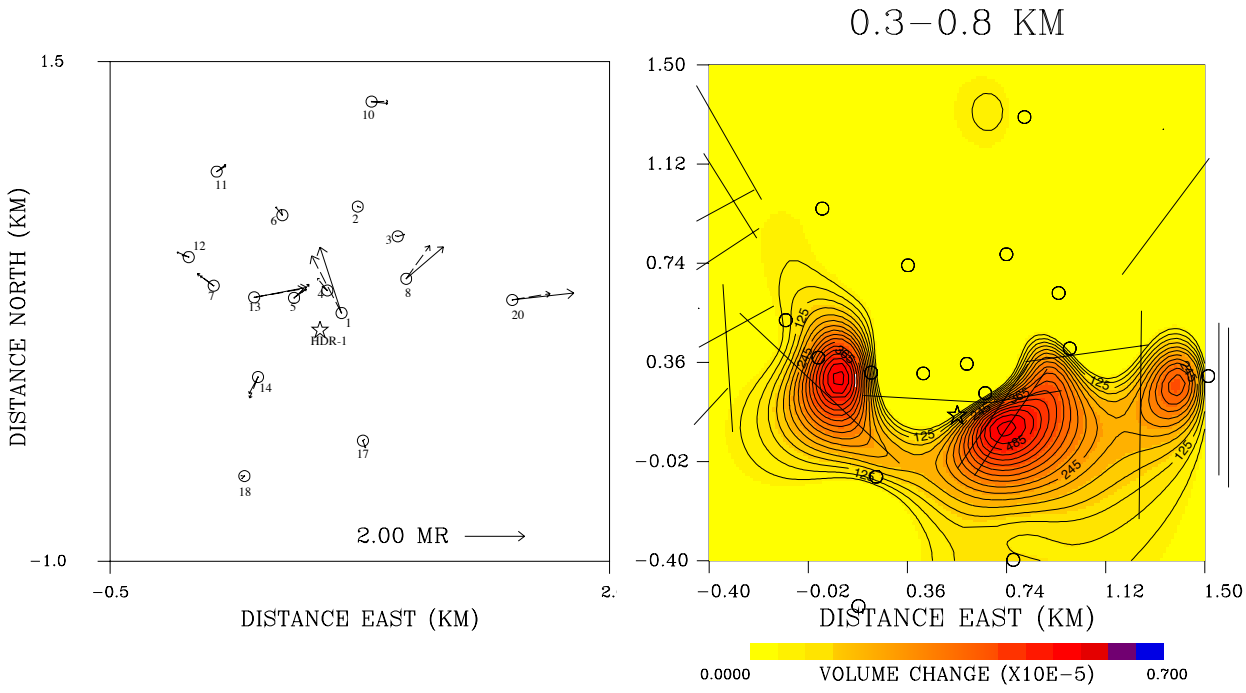

Figure 3. (Left) Tilt vectors associated with a network of 20 tilt meters used to monitor a deep injection in the well HDR-1 (indicated by a star). (Right) Network of tilt meters are indicated by open circles. Ring fractures from a caldera boundary are indicated by the solid lines. The color scale indicates the fractional volume change in the depth range 300 to 800 meters.

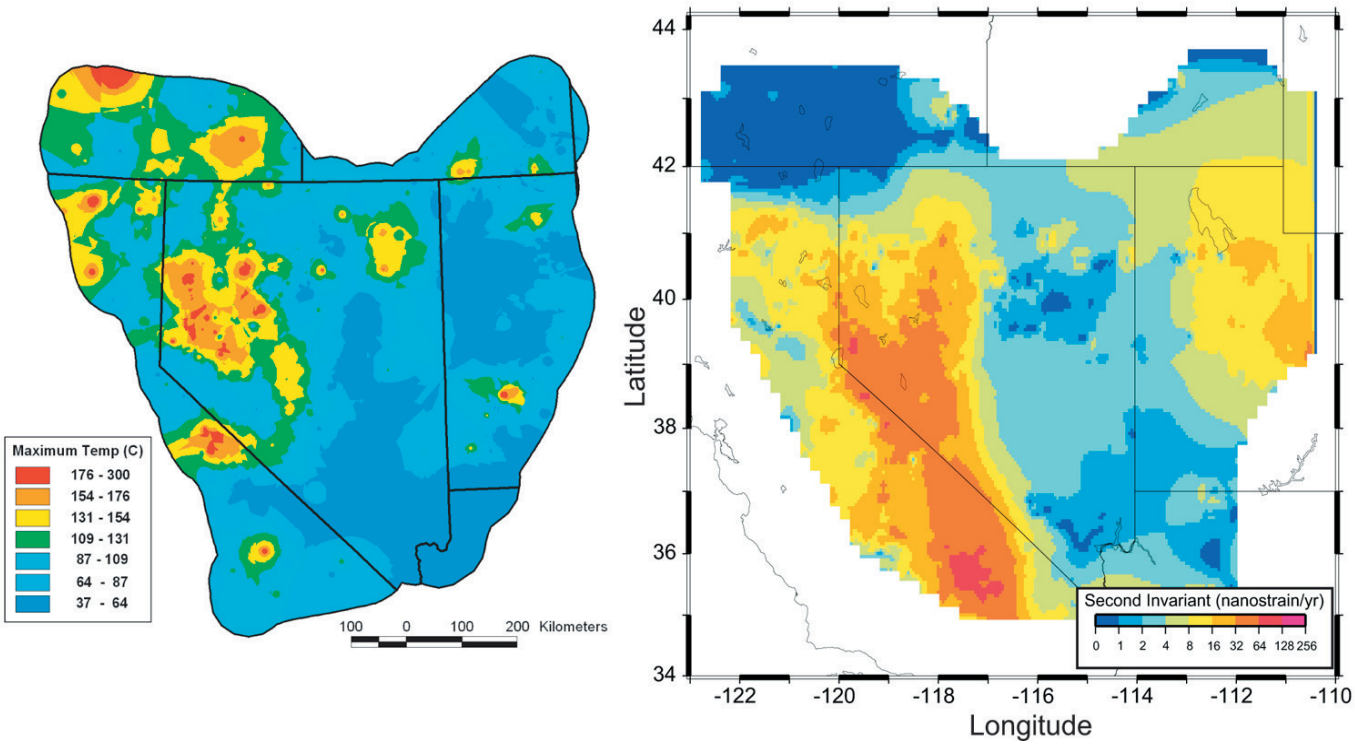

Figure 4. (Left) Color contours of maximum geothermal temperatures in Nevada. (Right) Magnitude of the crustal strain rate, the second strain invariant, in the Great Basin based upon available GPS data. From Blewitt et al. (2005).

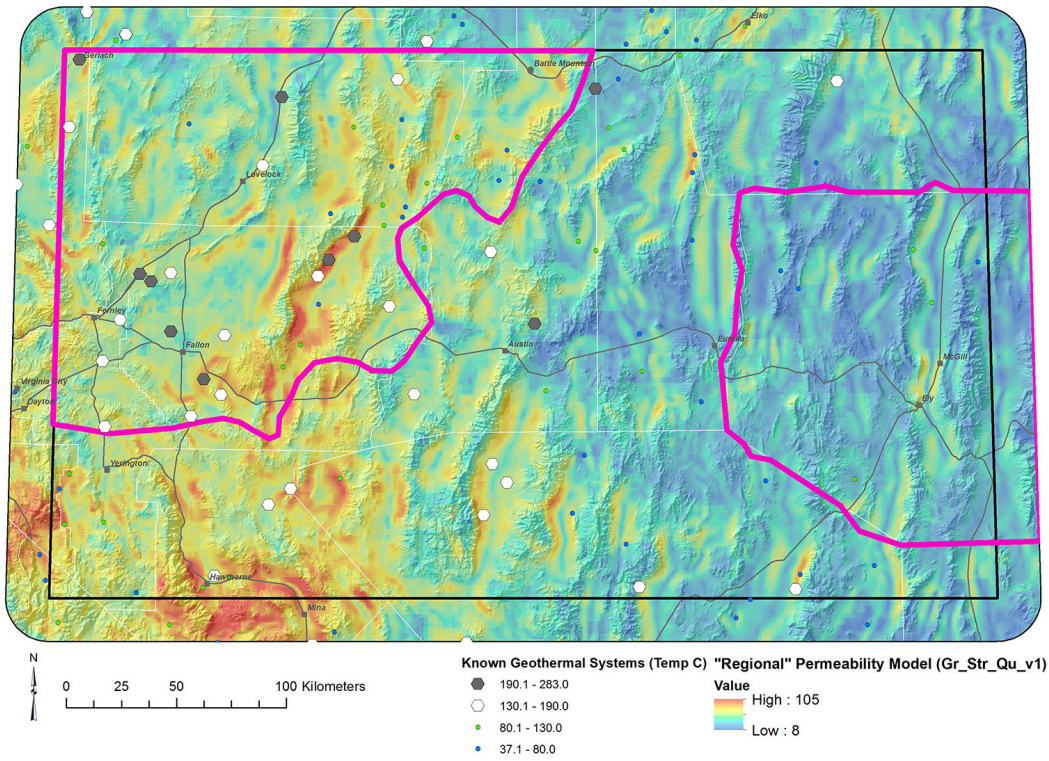

Figure 5. Permeability component of the play fairway score described in Faulds et al. (2018) obtained by combining GPS strain, gravity, and earthquake data.

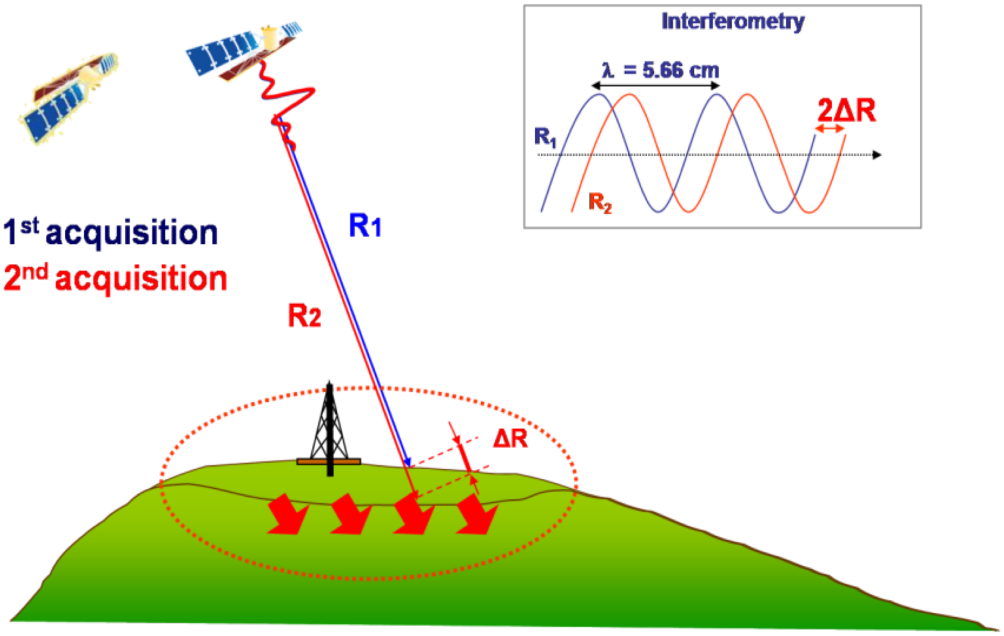

Figure 6. Principles underlying Interferometric Synthetic Aperture Radar (InSAR). Acquisitions at different times provide time series of microwave reflections from points on the Earth. If the surface characteristics do not change substantially, the phase shifts between the time series can be related to the change in line length, the range. The wavelength in the insert corresponds to InSAR in the C-band of the microwave spectrum.

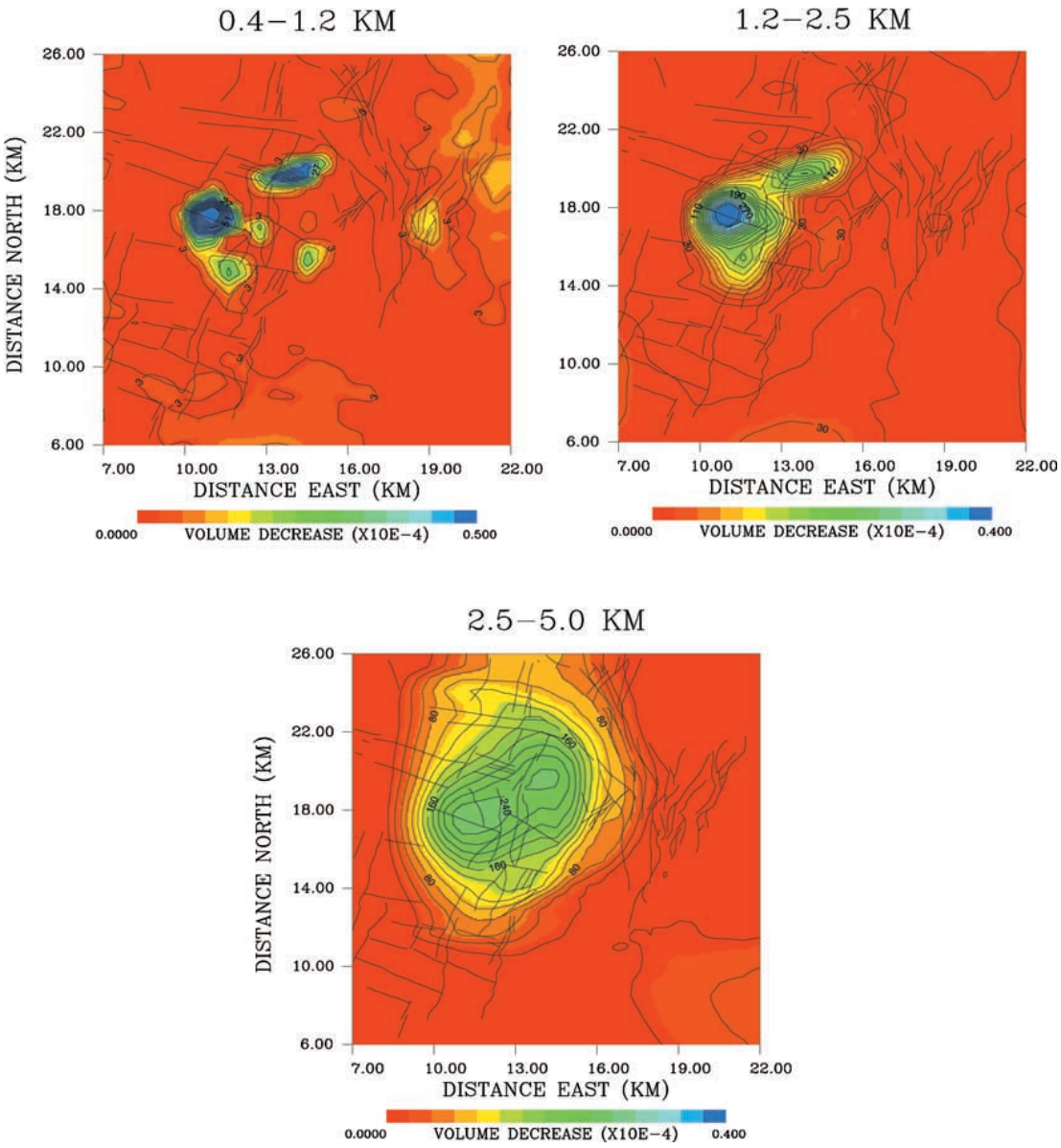

Figure 7. Reservoir volume change associated with geothermal production at the Coso geothermal field. From Vasco et al. 2002b.

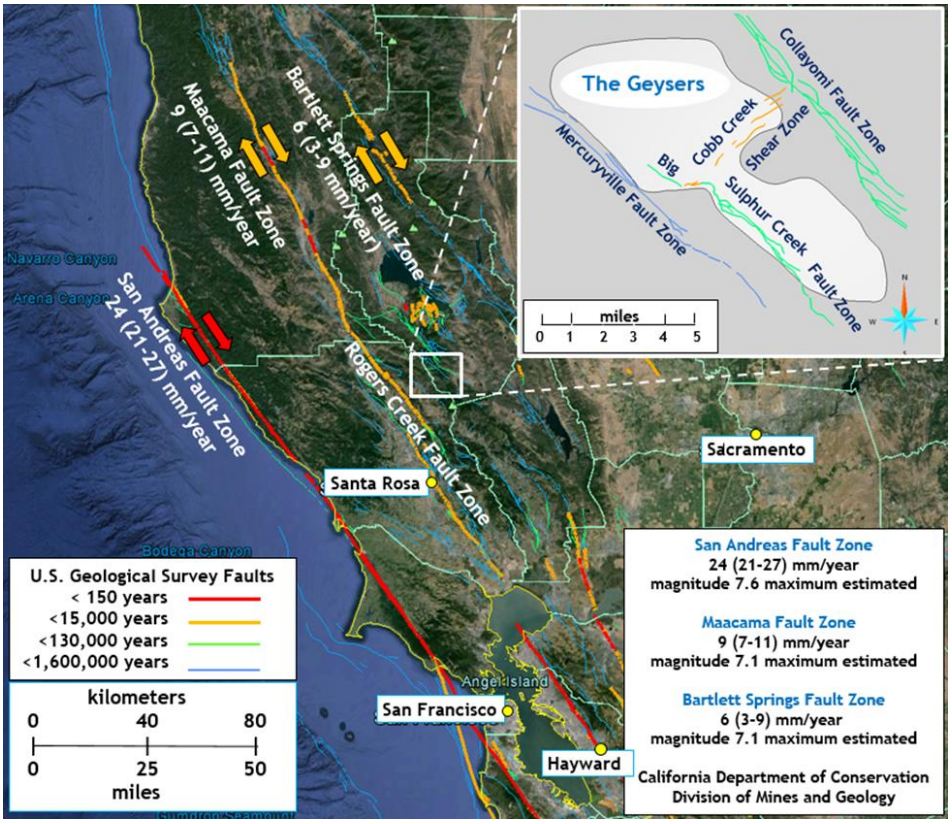

Figure 8. Location of The Geysers geothermal field in northern California. From Hartline et al. 2019, used with permission.

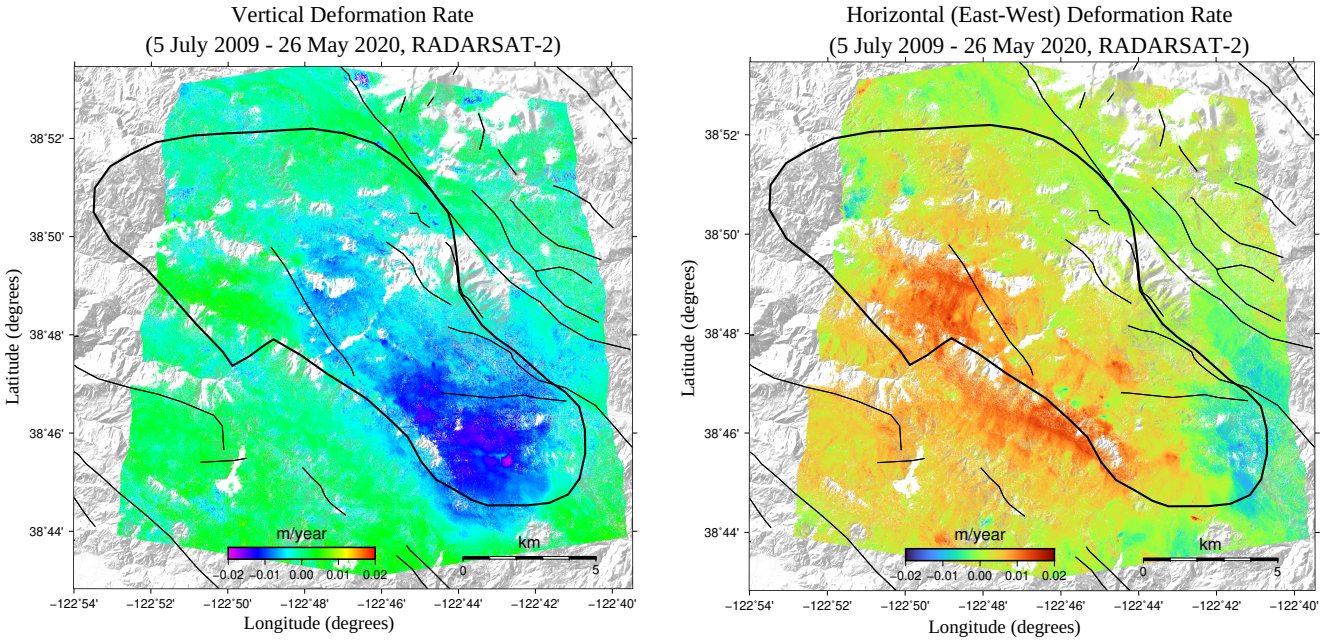

Figure 9. (Left). Rate of quasi-vertical deformation in velocities into vertical and east-west components utilizes both descending and ascending orbital data and assumes that the sensitivity meters/year. (Right). Rate of quasi-east-west deformation in meters/year. The decomposition of the to north-south motion can be neglected (Samsonov and d'Oreye, 2012).

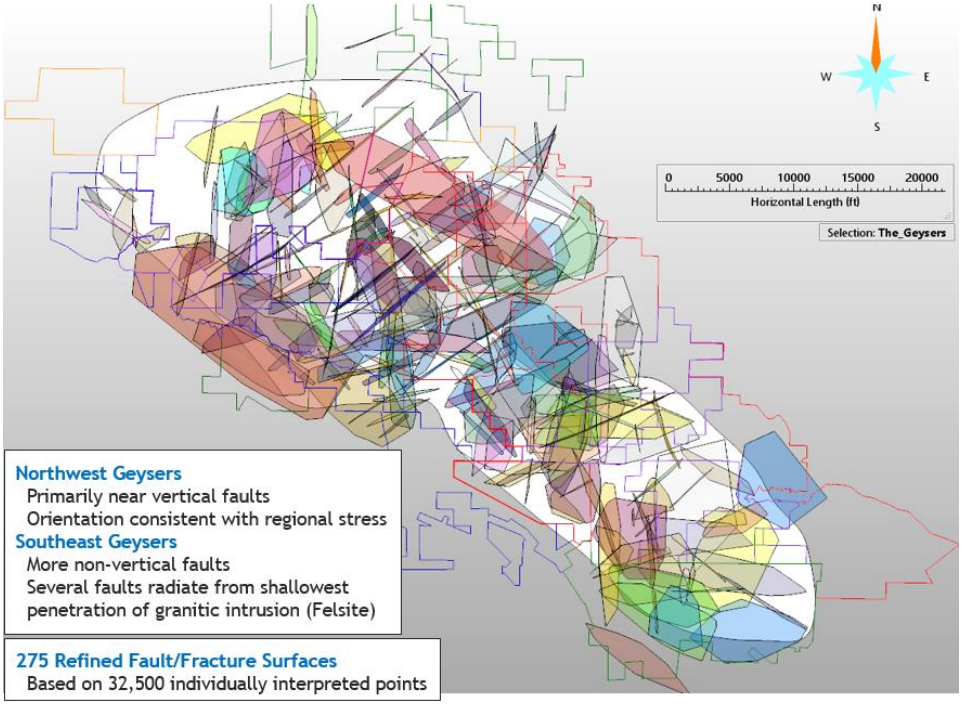

Figure 10. Refined fault surfaces within the main field of The Geysers (From Hartline et al. 2019).

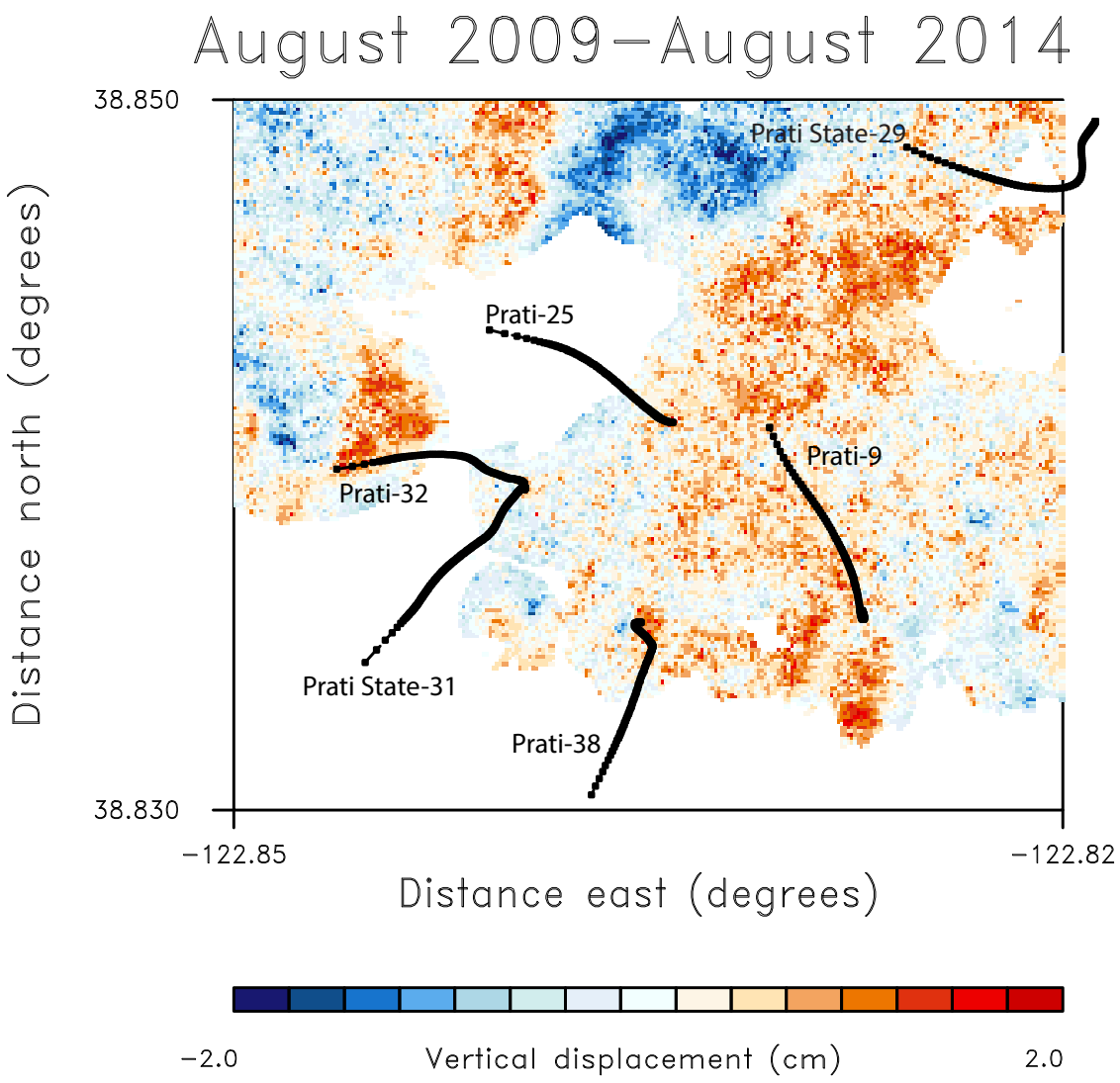

Figure 11. Quasi-vertical displacement derived from InSAR range change. The black lines denote the surface projections of well trajectories. The enhanced geothermal system (EGS) is between wells Prati-32 and Prati State-31.